IEEE Access
Multidisciplinary : Rapid Review : Open Access Journal

Received March 6, 2019, accepted May 12, 2019, date of publication May 17, 2019, date of current version June 4, 2019.

Digital Object Identifier 10.1109/ACCESS.2019.2917541

A Bayesian Framework for Joint Target Tracking, Classification, and Intent Inference

WANYING ZHANG, FENG YANG, AND YAN LIANG
School of Automation, Northwestern Polytechnical University, Xi'an 710072, China
Key Laboratory of Information Fusion Technology, Ministry of Education, Xi'an 710072, China

Corresponding author: Feng Yang (yangfeng@nwpu.edu.cn)

This work was supported in part by the National Science Foundation of China under Grant 61873205 and Grant 61374023, in part by the Natural Science Foundation of Shaanxi Province of China under Grant 2018MJ6048, and in part by the National Aerospace Science Foundation of China under Grant 20165153034.

ABSTRACT Intent inference has attracted considerable interest for achieving situation awareness in the high-level information fusion community. Different from traditional tracking-then-inference methods for intent inference, a novel scheme for joint target tracking, classification, and intent inference (JTCI) is developed based on the Bayesian framework. The proposed JTCI scheme exploits the dependence of target state on target class and intent by defining intent and class dependent dynamic model sets. Then, the joint target state, intent, and class density are obtained recursively under the assumption, and the kinematic and attribute measurement processes are conditional independent. Finally, simulations about tracking in the air surveillance system are utilized to demonstrate the superiority of the proposed JTCI to the state-of-the-art JTC.

INDEX TERMS Intent inference, situation awareness, joint target tracking, classification and intent inference, Bayesian framework.

I. INTRODUCTION

Information fusion refers to the process of data gathered from multiple sources to build a comprehensive view of the environment. As information fusion is ultimately performed for human needs, the commonly used Joint Director of Laboratories (JDL) model has been extended from low-level fusion process (e.g. target detection, tracking and classification) to high-level fusion process (e.g. situation awareness, impact assessment and process refinement) [1]–[7]. Recent years, in order to reduce tracking uncertainty there has been great interest in a joint tracking framework, which resolved different levels of fusion process, such as detection, classification and sensor management while tracking. Track before detect has been proposed for joint detection and tracking (JDT) of dim targets, where a number of consecutive scans are jointly processed without thresholding, and then the estimated target track is returned simultaneously as detection is declared [8]–[10]. Another JDT processing algorithm has been proposed for a multiple radar system, where the idea of feeding the information from the tracker to the detector is explored. The tracker can guide the detectors of multiple radars where to look for a target [11]. A joint data association and state estimation scheme has been developed based on the expectation-maximization framework, which is desirable to deal with the coupling issue of identification risk and estimation errors in over-the-horizon radar tracking system [12]. Joint target tracking and classification (JTC) is a popular framework for treating target tracking and classification problems jointly, which constructs the link between target state and class by incorporating class-dependent kinematic models [13]–[15]. Lately, several JTC based methods have been proposed to deal with the feasible implementation, computational efficiency, clutter environment, extended target and etc. In essence, classification is a decision problem. A joint decision and estimation framework has been proposed for solving the JTC problem based on a generalized Bayes risk considering both decision and estimation performance [16]–[18]. Furthermore, the problem of JTC within a sensor network has been studied in [19], where an optimal sensor selection scheme based on the maximization of the expected mutual information is integrated within the JTC framework. All the methods above indicate that a joint consideration of tracking and other levels of fusion process is more promising than a separate consideration.

In practice, a surveillance system concerns three questions: where and what the underlying target is, and what is it doing. The former two are related to tracking and classification,

The associate editor coordinating the review of this manuscript and approving it for publication was Mithun Mukherjee.

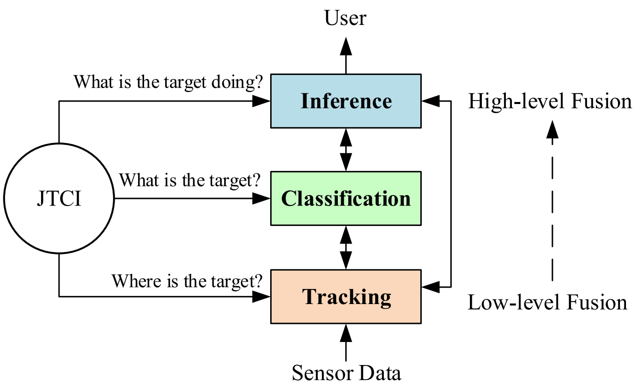

FIGURE 1. The JTCI illustration.

respectively, and the latter one corresponds to target intent inference. Intent inference is to interpret the motivations behind the actions that have just occurred. Moreover, target intent is an intersection of different levels of fusion process in the JDL fusion model [20], which plays an important role for integration of low and high levels of fusion. Conventional tracking systems solved intent inference in the tracking-then-inference style [6], [21]–[26]. It estimates the target tracks first and an inference is made based on this estimation. In fact, target tracking, classification and intent inference are three deeply coupled problems in a surveillance system as shown in Fig. 1. For example, class and intent determine the motion models which are essential for accurate tracking. At the same time, the target dynamics convey class and intent information. However, all the methods mentioned above deal with tracking and intent inference separately. Another types of methods, deep-learning based methods, use hierarchical abstract layers of latent variables to perform object recognition and classification. However, such methods lack theoretical foundations and do not capture model uncertainty. In comparison, probabilistic graphical models are more powerful and flexible with their Bayesian nature, which offer a mathematically grounded framework to make high-level inference and reason about model uncertainty. In addition, deep learning based methods often require a huge volume of labeled data and engineering experiences in neural network design, which cannot always be satisfied in practice. Therefore, it is highly demanded to develop the joint target tracking, classification and intent inference (JTCI) based on the Bayesian framework. Although the widely adopted JDL model defines a data process flow from low to high levels of fusion, no implemented framework is specified for JTCI.

In this paper, a novel scheme for JTCI based on the Bayesian framework is developed, considering the inter-dependence between tracking, classification and intent inference. By defining class and intent dependent motion models, an optimal Bayesian filter, named JTCI filter, is constructed to recursively propagate the joint state-intent-class probability density under the assumption that the kinematic and attribute measurement processes are conditional independent. At last, the proposed JTCI is applied to solve a tracking problem in the air surveillance system.

The rest of the paper is organized as follows. In Section II, the investigated problem is formulated. The JTCI scheme is developed in Section III, and then the performance of the JTCI is compared with the JTC in Section IV. Finally, conclusions are drawn in Section V.

II. PROBLEM FORMULATION

Consider the discrete-time dynamic system,

$$x_k = f(x_{k-1}, m_k) + w_{k-1}, \tag{1}$$

$$z_k^x = h(x_k) + v_k, \tag{2}$$

where x_k and z_k^x represent the state vector and the kinematic measurement vector at time k, respectively, f is the state function, h is the kinematic sensor (e.g. radar) function. w_k and v_k are the uncorrelated zero-mean Gaussian white process and measurement noises with covariance matrices Q_k and R_k, respectively. The motion model m_k follows a finite-state, first-order Markov chain and takes values from a finite set $M = \{m_1, \ldots m_N\}$ [27].

The measurement process of an attribute sensor, e.g. electronic support measure (ESM), is obtained from the confusion and the emitter usage transition matrices. For more details, see [13]. Here, it is concisely represented by

$$p(z_k^c|c) = p_c(z_k^c - c), \tag{3}$$

where $c \in \{1, 2, \ldots, C\}$ represents the target class, z_k^c is the class measurement, and p_c is the target class probability determined from the class measurement.

In addition, it is assumed that z_k^c is only statistically dependent of target class c and z_k^x is only statistically dependent of target state x_k [13] [28].

As shown in Fig. 2, the existing JTC framework [13] has been presented for the case that m_k is only class-dependent. Here, the model transition probability at time k is defined as

$$p_k^{i|j} = \Pr(m_k = m_i | m_{k-1} = m_j, c), \quad i, j = 1, \ldots, N, \tag{4}$$

In practice, targets in the scene do not move randomly [29]. Instead, they usually follow specific motion patterns not only according to their classes (e.g. airliner, bomber and fighter) but also their intents (e.g. cruise, attack and escape). For example, a cruising airliner may imply constant velocity motion model, while an attacking fighter may imply strong maneuver. Therefore, incorporating intent into dynamic modeling would be more promising in reducing the tracking uncertainty. However, learning and inferring intent is a non-trivial job:

- The stationarity assumption of target class has been favored for its simplicity in most applications of JTC so far. However, this assumption is not always valid for intent inference. For example, a pilot will change his intent according to different combat situations.
- Attribute sensors, such as ESM, can identify the likely source emitters carried on board to assist classification,

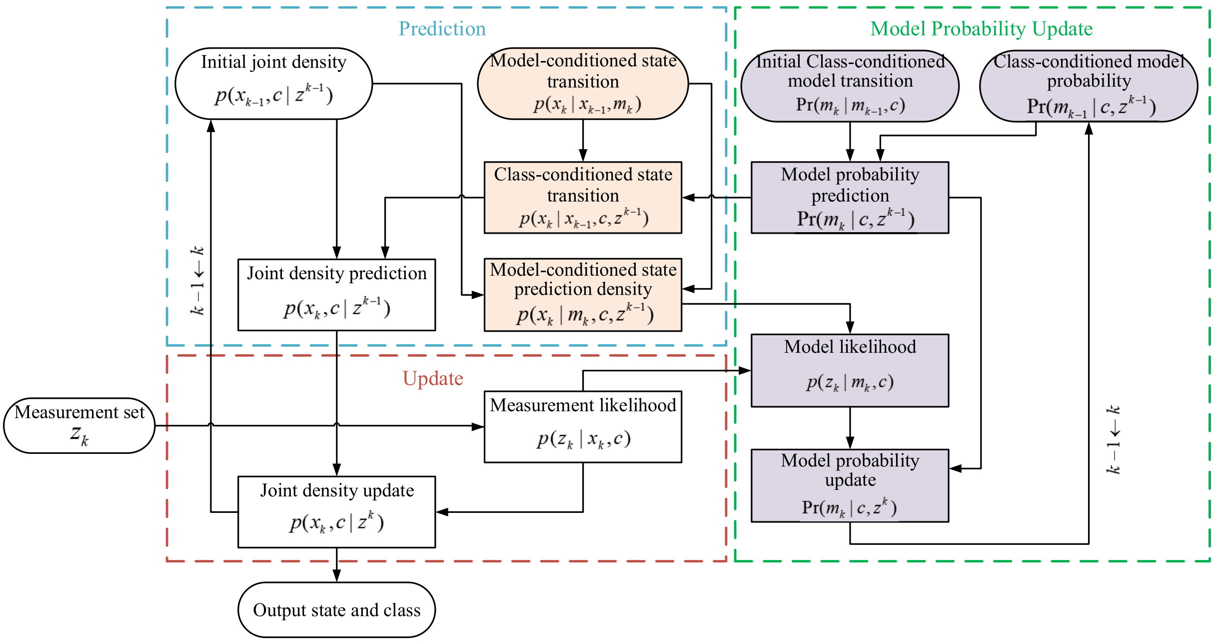

FIGURE 2. Diagram of the existing JTC framework.

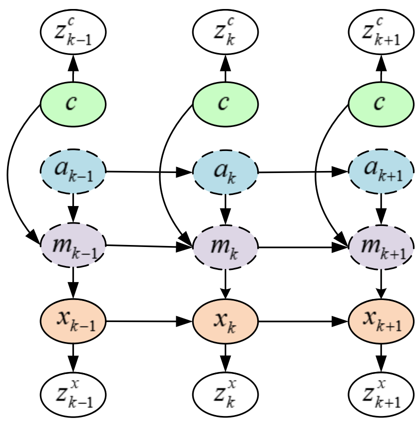

FIGURE 3. Graphical representation of the variable interdependencies over time.

while there is no way to observe the intent directly. Intent is hidden in nature and can only be inferred via other observable variables.

Considering the fact that the motion model transition of a certain kind of target is to perform some intent, we present the class and intent dependent dynamic models as depicted in Fig. 3, where each circle represents a node, the latent nodes are shown in dashed circles, and the black edges express probabilistic dependency among nodes. The model transition probability matrix is defined by

$$\pi_k^{ij} = \Pr(m_k = m_i \mid m_{k-1} = m_j, a_k, c), \quad i, j = 1, \ldots, N_{ac}, \tag{5}$$

where $a_k \in \{1, 2, .., A\}$ is the target intent at time k. We assume that the intent is evolving according to a first-order Markov chain with a known transition probability $\Pr(a_k \mid a_{k-1})$. It is noted that the number of models N_{ac} may be different for each pair of class and intent.

The objective of this paper is to recursively calculate the posterior joint state-intent-class density $p(x_k, a_k, c \mid z^k)$ for the system in (1)–(3), where $z^k = \{z_1, .., z_k\}$ is the set of measurements up to time k and $z_k = \{z_k^x, z_k^c\}$ represents the set of kinematic and class measurements at time k.

III. JOINT TARGET TRACKING, CLASSIFICATION AND INTENT INFERENCE

The uncertainty about the state, class and intent of a target is jointly described by the posterior joint state-intent-class density,

$$p(x_k, a_k, c \mid z^k), \quad c \in \{1, 2, \ldots, C\}, \; a_k \in \{1, 2, \ldots, A\}, \tag{6}$$

which satisfies

$$\sum_{a_k} \sum_{c} \int p\,(x_k, a_k, c \mid z^k)\, dx_k = 1. \tag{7}$$

The following theorems provide the recursions for the joint density, named the JTCI filter.

Theorem 1 (Joint Density Prediction): Given the posterior joint state-intent-class density $p(x_{k-1}, a_{k-1}, c \mid z^{k-1})$ at time $k-1$, the predicted joint density at time k is given by

$$\begin{aligned} p(x_k, a_k, c \mid z^{k-1}) &= \sum_{a_{k-1}} \int p(x_k \mid x_{k-1}, a_k, c, z^{k-1}) \\ &\quad \times \Pr(a_k \mid a_{k-1}) p(x_{k-1}, a_{k-1}, c \mid z^{k-1}) dx_{k-1}, \end{aligned} \tag{8}$$

with

$$p(x_k|x_{k-1}, a_k, c, z^{k-1}) = \sum_{m_k} p(x_k|x_{k-1}, m_k) \Pr(m_k|a_k, c, z^{k-1}), \tag{9}$$

$$\Pr(m_k|a_k, c, z^{k-1}) = \sum_{m_{k-1}} \Pr(m_k|m_{k-1}, a_k, c) \times \sum_{a_{k-1}} \Pr(m_{k-1}|a_{k-1}, c, z^{k-1}) \Pr(a_{k-1}|a_k, z^{k-1}), \tag{10}$$

$$\Pr(a_{k-1}|a_k, z^{k-1}) = \frac{\Pr(a_k|a_{k-1}) \Pr(a_{k-1}|z^{k-1})}{\Pr(a_k|z^{k-1})}, \tag{11}$$

$$\Pr(a_k|z^{k-1}) = \sum_{a_{k-1}} \Pr(a_k|a_{k-1}) \Pr(a_{k-1}|z^{k-1}), \tag{12}$$

where $p(x_k|x_{k-1}, a_k, c, z^{k-1})$ is the intent and class conditioned state transition density, $p(x_k|x_{k-1}, m_k)$ is the model-conditioned state transition density, $\Pr(m_k|a_k, c, z^{k-1})$ is the model prediction probability, and $\Pr(a_k|z^{k-1})$ is the intent prediction probability. $\Pr(m_{k-1}|a_{k-1}, c, z^{k-1})$ and $\Pr(a_{k-1}|z^{k-1})$ are the model and intent posterior probabilities at time $k-1$, respectively.

Proof: See Appendix A. ■

Theorem 2 (Joint Density Update): Given the predicted joint density as shown in (8), then the joint posterior density is given by

$$p(x_k, a_k, c|z^k) = \frac{1}{\delta_k} p\,(z_k|x_k, a_k, c) p(x_k, a_k, c|z^{k-1}), \tag{13}$$

with

$$p(z_k|x_k, a_k, c) = p(z_k^x|x_k) p(z_k^c|c), \tag{14}$$

$$p(z_k^x|x_k) = p_w(z_k^x - h(x_k)), \tag{15}$$

where $\delta_k = \sum_c \sum_{a_k} \int p(z_k|x_k, a_k, c) p(x_k, a_k, c|z^{k-1}) dx_k$ is a normalization factor, p_w is the density of the measurement noise in (2), and $p(z_k^c|c)$ is given in (3).

Proof: See Appendix B. ■

Theorem 3 (Model Probability Update): The class and intent dependent model probability is evaluated as

$$\Pr(m_k|a_k, c, z^k) = \frac{1}{\sigma_k} p(z_k|m_k, a_k, c, z^{k-1}) \times \Pr(m_k|a_k, c, z^{k-1}), \tag{16}$$

with

$$p(z_k|m_k, a_k, c, z^{k-1}) = \int p(z_k^e|c) p(z_k^r|x_k) \times p(x_k|m_k, a_k, c, z^{k-1}) dx_k, \tag{17}$$

$$p(x_k|m_k, a_k, c, z^{k-1}) = \int p(x_k|x_{k-1}, m_k) \times \sum_{a_{k-1}} p(x_{k-1}|a_{k-1}, c, z^{k-1}) \times \Pr(a_{k-1}|a_k, z^{k-1}) dx_{k-1}, \tag{18}$$

where $\sigma_k = \sum_{m_k} p(z_k|m_k, a_k, c, z^{k-1}) \Pr(m_k|a_k, c, z^{k-1})$ is the normalizing constant, $p(z_k|m_k, a_k, c, z^{k-1})$ is the model likelihood, and $p(x_k|m_k, a_k, c, z^{k-1})$ is the model conditioned state prediction density.

Proof: See Appendix B. ■

Output: Substitute (14) and (8) into (13), we can compute the intent posterior probability by integrating the joint density over the state and class,

$$\Pr(a_k|z^k) = \sum_c \int p(x_k, a_k, c|z^k) dx_k = \frac{1}{\delta_k} \sum_c \int p(z_k^r|x_k) p(z_k^e|c) p(x_k|a_k, c, z^{k-1}) \times p(c|z^{k-1}) dx_k \Pr(a_k|z^{k-1}). \tag{19}$$

Similarly, the class posterior probability is evaluated as

$$\Pr(c|z^k) = \sum_{a_k} \int p(x_k, a_k, c|z^k) dx_k = \frac{1}{\delta_k} \sum_{a_k} \int p(z_k^r|x_k) p(z_k^e|c) p(x_k|a_k, c, z^{k-1}) \times p(a_k|z^{k-1}) dx_k \Pr(c|z^{k-1}), \tag{20}$$

where the intent and class conditioned state density on the right hand side of (19) and (20) can be reexpressed as

$$p(x_k|a_k, c, z^{k-1}) = \frac{p(x_k, a_k, c|z^{k-1})}{\int p(x_k, a_k, c|z^{k-1}) dx_k}. \tag{21}$$

Finally, we can compute the state estimate with respect to the commonly used minimum mean square error criterion. The state estimate for each class $c = i$ and intent $a_k = j$ is

$$\hat{x}_{k|k}^{ij} = \int x_k p(x_k, a_k = j, c = i|z^k) dx_k, \quad i \in \{1, 2, \ldots, C\}, \quad j \in \{1, 2, \ldots, A\}, \tag{22}$$

which takes part in the combined state estimate

$$\hat{x}_{k|k} = \sum_i \sum_j \hat{x}_{k|k}^{ij} \Pr(a_k = j|z^k) \Pr(c = i|z^k). \tag{23}$$

According to Theorems 1-3, the proposed JTCI with class and intent dependent dynamic model is shown in Fig. 4.

Remark 1: As seen from Figs. 2 and 4, the differences between the proposed JTCI and the existing JTC are: (1) the JTCI adds the intent transition in the prediction step while the existing JTC does not need to do this, and (2) the JTCI considers the effect of target intent on model transition, while the model transition in JTC is only class-dependent, and (3) the JTC does not provide information on target intent while the JTCI can output the intent probability, which will assist the commander to take timely actions against potential threats.

If the state function f in (1) and measurement function h in (2) are all linear, then the integrals in Theorems 1-3 can be accurately evaluated by linear transformation. As for the

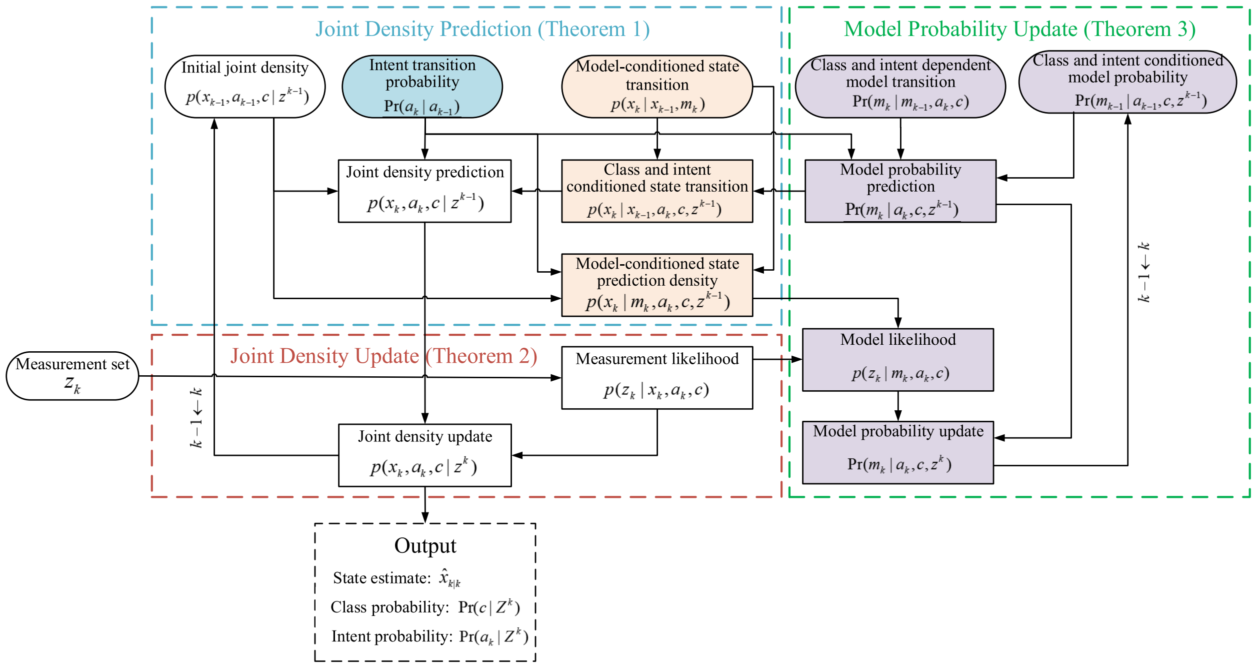

FIGURE 4. Diagram of the proposed JTCI.

nonlinear f and h, the analytical solution will not be available in general. Therefore, it is necessary to resort to some numerically approximate methods, such as the linearization [30], unscented transformation [31] and sampling based methods [32].

IV. SIMULATION

In this section, we will demonstrate the effectiveness of the proposed JTCI, and compare its performance with the JTC [13]. Two tracking scenarios are considered as shown in Figs. 5 and 6, including a weak-maneuvering aircraft (class 1), such as a military cargo aircraft and a high-maneuvering aircraft (class 2), such as a fighter. The target is assumed to behave different intents including cruise (intent 1) and attack (intent 2) during the flight. The maneuver is modeled as acceleration changes in the kinematic model. Here, suppose that the target state vector $x_k = [\xi_k, \dot{\xi}_k, \eta_k, \dot{\eta}_k]^T$ is comprised of position (ξ_k, η_k) and velocity $(\dot{\xi}_k, \dot{\eta}_k)$, the state transition function in (1) is given by $x_{k+1} = F_k x_k + G m_k + v_k$ with

$$F_k = I_2 \otimes \begin{bmatrix} 1 & T \\ 0 & 1 \end{bmatrix}, \quad G = I_2 \otimes \begin{bmatrix} \frac{T^2}{2} \\ T \end{bmatrix},$$

where $T = 1$s is the sampling interval and 90 steps are run in the simulation. The maneuver input $m_k = [a_{x,k}, a_{y,k}]^T$ includes accelerations along x and y coordinates.

Radar and ESM are located at the origin of the Cartesian coordinate system. We assume that radar measurements are synchronized and have been associated with the ESM measurements. The radar function in (2) is $h(x_k) = [\xi_k, \eta_k]^T$ with $R = diag(\sigma_x^2, \sigma_y^2)$, where $\sigma_x = \sigma_x = 100$ m.

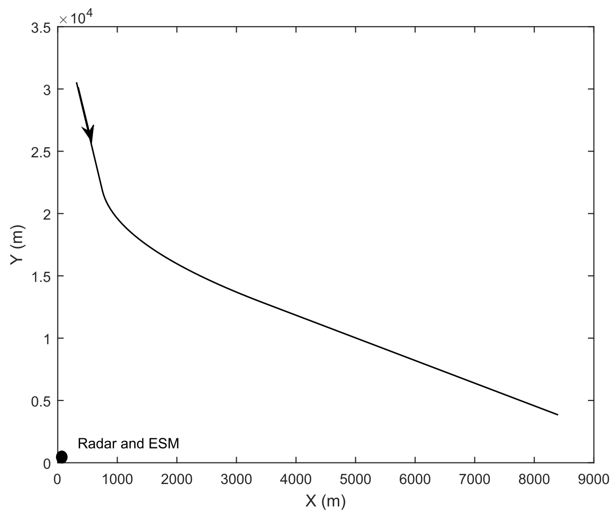

FIGURE 5. The true trajectory in Scenario 1.

The ESM declaration sequence in (3) is based on the same emitter usage Markov chains, detection probabilities and confusion matrix as in [13].

Scenario 1: Consider a cruising military cargo as shown in Fig. 5. It flies at a constant velocity (CV) of [15,−300] m/s from [300,30840] km between 0 s and 30 s. Then, it performs a course change with a 5 g maneuver between 30 s and 60 s. Next it continues at CV motion for the completion of the trajectory.

Scenario 2: This scenario is a high maneuvering fighter with time-varying intent, see Fig. 6. Consider a fighter cruises at a CV of [−8.3,−399.9] m/s from [41689,40840] km between 0 s and 15 s. Suddenly, it spots threats and performs

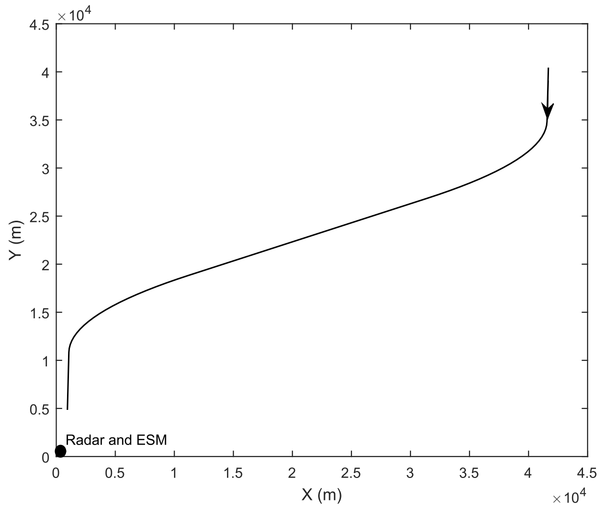

FIGURE 6. The true trajectory in scenario 2.

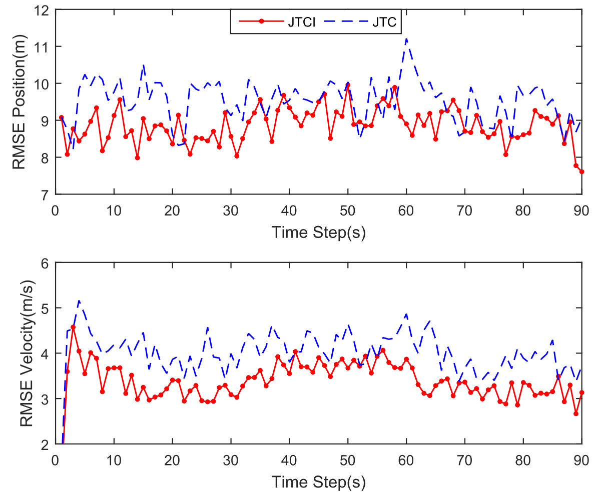

FIGURE 7. Performance comparison in scenario 1.

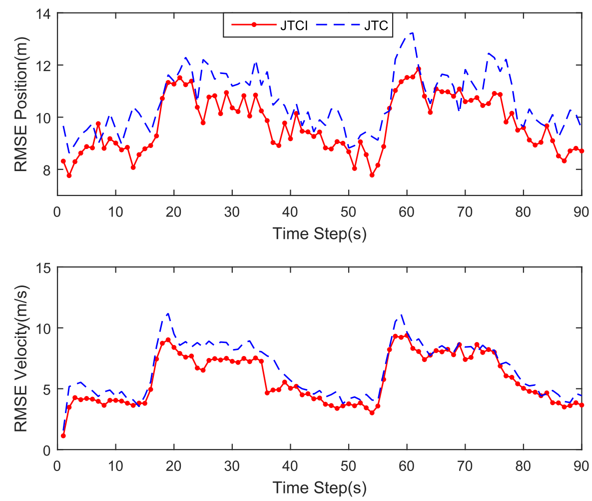

FIGURE 8. Performance comparison in scenario 2.

an attack with a -5 g maneuver between 15 s and 35 s. After cruising between 35 s and 55 s, the fighter discovers threats again and performs an attack with a 5 g maneuver between 55 s and 75 s. With the disappearance of threat, it resumes cruising at CV motion for the completion of the trajectory.

For the JTCI, the initial class and intent probabilities are $\Pr(c = i|z_0) = 0.5, \Pr(a_0 = j|z_0) = 0.5 (i, j = 1, 2)$. The intent transition probability is given by $T_a = [0.95\ 0.05; 0.05\ 0.95]$. The acceleration process m_k for class c and intent a_k is assumed to be belong to model set M^{ca_k}, $c \in \{1, 2\}$, $a_k \in \{1, 2\}$ and

$$\begin{aligned}
&M_1^{11} = [0, 0]^T, \quad M_2^{11} = [-0.5g, 0]^T, \ M_3^{11} = [0.5g, 0]^T,\\
&M_1^{12} = [0, 0]^T, \quad M_2^{12} = [-1g, 0]^T, \ M_3^{12} = [1g, 0]^T,\\
&M_1^{21} = [0, 0]^T, \quad M_2^{21} = [-1g, 0]^T, \ M_3^{21} = [1g, 0]^T,\\
&M_1^{22} = [0, 0]^T, \quad M_2^{22} = [-5g, 0]^T, \ M_3^{22} = [5g, 0]^T.
\end{aligned}$$

The initial class and intent conditioned model probabilities are $\Pr(m_0|c = i, a_0 = j, z_0) = 1/3\ (i, j = 1, 2)$. The model transition matrix is set according to the intent and class:

$$\pi^{11} = \begin{bmatrix} 0.9 & 0.05 & 0.05 \\ 0.05 & 0.9 & 0.05 \\ 0.05 & 0.05 & 0.9 \end{bmatrix}, \quad \pi^{12} = \begin{bmatrix} 0.8 & 0.1 & 0.1 \\ 0.2 & 0.8 & 0 \\ 0.2 & 0 & 0.8 \end{bmatrix},$$
$$\pi^{21} = \begin{bmatrix} 0.9 & 0.05 & 0.05 \\ 0.05 & 0.9 & 0.05 \\ 0.05 & 0.05 & 0.9 \end{bmatrix}, \quad \pi^{22} = \begin{bmatrix} 0.4 & 0.3 & 0.3 \\ 0.5 & 0.5 & 0 \\ 0.5 & 0 & 0.5 \end{bmatrix}.$$

For the JTC, the acceleration input for class c is assumed to be belong to model set M^c, $c \in \{1, 2\}$ and

$$\begin{aligned}
&M_1^1 = [0, 0]^T, \quad M_2^1 = [-0.5g, 0]^T, \ M_3^1 = [0.5g, 0]^T,\\
&M_4^1 = [-1g, 0]^T, \quad M_5^1 = [1g, 0]^T,\\
&M_1^2 = [0, 0]^T, \quad M_2^2 = [-1g, 0]^T, \ M_3^2 = [1g, 0]^T,\\
&M_4^2 = [-5g, 0]^T, \quad M_5^2 = [5g, 0]^T.
\end{aligned}$$

The initial class conditioned model probabilities are $\Pr(m_0|c = i, z_0) = 1/5\ (i = 1, 2)$. The model transition matrix is given by

$$\pi^i = \begin{bmatrix} 0.8 & 0.05 & 0.05 & 0.05 & 0.05 \\ 0.05 & 0.8 & 0 & 0.05 & 0 \\ 0.05 & 0 & 0.8 & 0 & 0.05 \\ 0.05 & 0.05 & 0 & 0.8 & 0 \\ 0.05 & 0 & 0.05 & 0 & 0.8 \end{bmatrix}$$

for both classes.

The root mean-squared errors (RMSEs) on position and speed, average probabilities of class and intent are chosen as metrics to evaluate the performance.

Figs. 7–8 show the comparison results over 100 Monte Carlo runs for the two scenarios. Table 1 lists the estimation accuracy in terms of RMSEs for position and velocity of JTCI and JTC after being implemented for 10 s (to reduce the effects of initialization). It can be seen that the JTCI outperforms the JTC in terms of position and velocity accuracy and the JTCI provides lower peak errors than the JTC in the two scenarios. This is because that the proposed JTCI can

TABLE 1. Estimation accuracy of JTC and JTCI.

	APE (m)	PPE (m)	AVE (m/s)	PVE (m/s)
		Scenario 1		
JTC	9.61	11.21	4.67	4.87
JTCI	8.86	9.95	3.38	4.01
		Scenario 2		
JTC	11.23	13.23	6.57	11.19
JTCI	9.74	11.85	5.77	9.31

[1] APE = average position error
PPE = peak position error
AVE = average velocity error
PVE = peak velocity error

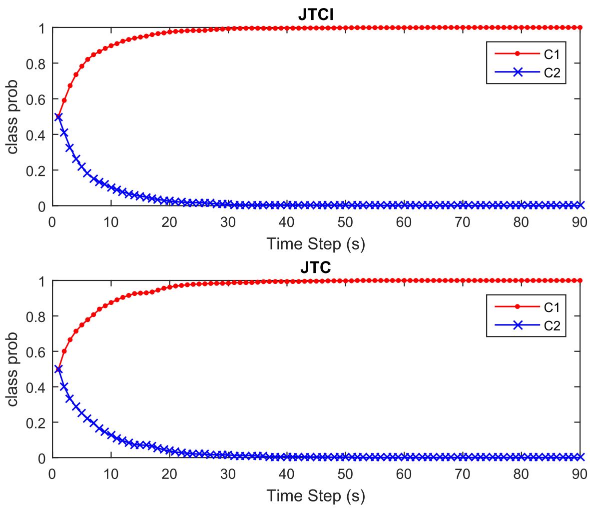

FIGURE 9. Class probabilities in scenario 1.

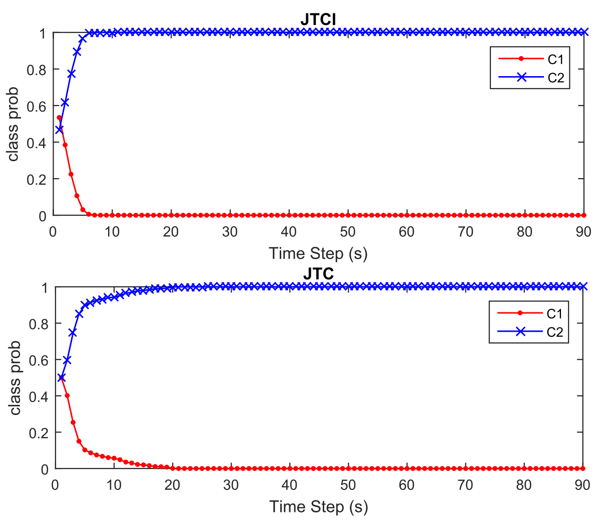

FIGURE 10. Class probabilities in scenario 2.

accommodate more realistic situations in which a class of targets with different intents may have different kinematic model sets, while the JTC does not consider this information

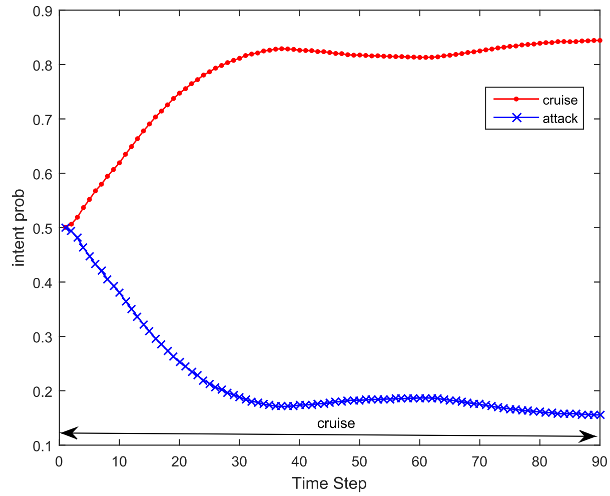

FIGURE 11. Intent probabilities for JTCI in scenario 1.

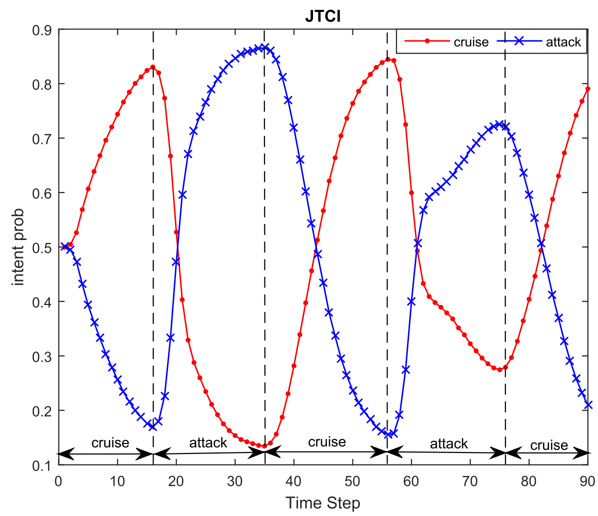

FIGURE 12. Intent probabilities for JTCI in scenario 2.

and assumes that a class of targets have the same kinematic model set.

Figs. 9-10 show the class probabilities for the two scenarios. Both the JTCI and JTC output correct classifications with radar and ESM measurements. Besides, the intent probabilities estimated by the proposed JTCI are presented in Figs. 11-12. It is observed that intents with larger estimated probabilities at different time steps are closely consistent with the ground truth as shown at the bottom of Figs. 11-12.

In addition, the calculation time for each recursion of the JTCI and JTC are 0.0017 s and 0.0015 s, respectively. As a result, the JTCI is superior to the JTC, but has a slightly higher computational cost than the JTC.

V. CONCLUSIONS

By the fact that the motion model is not only determined by target class, but also target intent, a JTCI is proposed in this paper. It is obtained via recursively propagating the joint density of state, class and intent based on the Bayesian framework. The simulation indicates that the proposed method outperforms the existing JTC by its superior estimation accuracy, correct target classification and intent inference.

APPENDIX A

Joint density prediction:

$$\begin{aligned} p(x_k, a_k, c|z^{k-1}) &= \sum_{a_{k-1}} \int p(x_k, a_k, c, x_{k-1}, a_{k-1}, z^{k-1}) dx_{k-1} \\ &= \sum_{a_{k-1}} \int p(x_k|a_k, c, x_{k-1}, a_{k-1}, z^{k-1}) \\ &\quad \times p(a_k|c, x_{k-1}, a_{k-1}, z^{k-1}) p(x_{k-1}, a_{k-1}, c|z^{k-1}) dx_{k-1} \\ &= \sum_{a_{k-1}} \int p(x_k|x_{k-1}, a_k, c, z^{k-1}) p(a_k|a_{k-1}) \\ &\quad \times p(x_{k-1}, a_{k-1}, c|z^{k-1}) dx_{k-1} \end{aligned} \tag{24}$$

Class and intent conditioned state transition density:

$$\begin{aligned} p(x_k|x_{k-1}, a_k, c, z^{k-1}) &= \sum_{m_k} p(x_k|x_{k-1}, m_k, a_k, c, z^{k-1}) \Pr(m_k|x_{k-1}, a_k, c, z^{k-1}) \\ &= \sum_{m_k} p(x_k|x_{k-1}, m_k) \Pr(m_k|a_k, c, z^{k-1}) \end{aligned} \tag{25}$$

Model probability prediction:

$$\begin{aligned} \Pr(m_k|a_k, c, z^{k-1}) &= \sum_{m_{k-1}} \Pr(m_k|m_{k-1}, a_k, c, z^{k-1}) \Pr(m_{k-1}|a_k, c, z^{k-1}) \\ &= \sum_{m_{k-1}} \Pr(m_k|m_{k-1}, a_k, c) \sum_{a_{k-1}} \Pr(m_{k-1}|a_{k-1}, c, z^{k-1}) \\ &\quad \times \Pr(a_{k-1}|a_k, z^{k-1}) \end{aligned} \tag{26}$$

APPENDIX B

Intent probability update:

$$\begin{aligned} \Pr(a_k|z^k) &= \sum_c \int p(x_k, a_k, c|z^k) dx_k \\ &= \frac{1}{\delta_k} \sum_c \int p(z_k^r|x_k) p(z_k^e|c) p(x_k, a_k, c|z^{k-1}) dx_k \\ &= \frac{1}{\delta_k} \sum_c \int p(z_k^r|x_k) p(z_k^e|c) p(x_k|a_k, c, z^{k-1}) \\ &\quad \times p(c|z^{k-1}) dx_k p(a_k|z^{k-1}) \end{aligned} \tag{27}$$

Class probability update:

$$\begin{aligned} \Pr(c|z^k) &= \sum_{a_k} \int p(x_k, a_k, c|z^k) dx_k \\ &= \frac{1}{\delta_k} \sum_{a_k} \int p(z_k^r|x_k) p(z_k^e|c) p(x_k, a_k, c|z^{k-1}) dx_k \\ &= \frac{1}{\delta_k} \sum_{a_k} \int p(z_k^r|x_k) p(z_k^e|c) p(x_k|a_k, c, z^{k-1}) \\ &\quad \times p(a_k|z^{k-1}) dx_k p(c|z^{k-1}) \end{aligned} \tag{28}$$

Model probability update:

$$\begin{aligned} p(z_k|m_k, a_k, c, z^{k-1}) &= \int p(z_k, x_k|m_k, a_k, c, z^{k-1}) dx_k \\ &= \int p(z_k^e|c) p(z_k^r|x_k) \\ &\quad \times p(x_k|m_k, a_k, c, z^{k-1}) dx_k \end{aligned} \tag{29}$$

$$\begin{aligned} p(x_k|m_k, a_k, c, z^{k-1}) &= \int p(x_k|x_{k-1}, m_k, a_k, c, z^{k-1}) \\ &\quad \times p(x_{k-1}|m_k, a_k, c, z^{k-1}) dx_{k-1} \\ &= \int p(x_k|x_{k-1}, m_k) p(x_{k-1}|a_k, c, z^{k-1}) dx_{k-1} \\ &= \int p(x_k|x_{k-1}, m_k) \sum_{a_{k-1}} p(x_{k-1}|a_{k-1}, a_k, c, z^{k-1}) \\ &\quad \times \Pr(a_{k-1}|a_k, c, z^{k-1}) dx_{k-1} \\ &= \int p(x_k|x_{k-1}, m_k) \sum_{a_{k-1}} p(x_{k-1}|a_{k-1}, c, z^{k-1}) \\ &\quad \times \Pr(a_{k-1}|a_k, z^{k-1}) dx_{k-1} \\ &= \int p(x_k|x_{k-1}, m_k) \sum_{a_{k-1}} p(x_{k-1}|a_{k-1}, c, z^{k-1}) \\ &\quad \times \Pr(a_{k-1}|a_k, z^{k-1}) dx_{k-1}, \end{aligned} \tag{30}$$

where the intent and class conditioned prior state density on the right hand side above can be reexpressed as

$$p(x_{k-1}|a_{k-1}, c, z^{k-1}) = \frac{p(x_{k-1}, a_{k-1}, c|z^{k-1})}{\int p(x_{k-1}, a_{k-1}, c|z^{k-1}) dx_{k-1}}. \tag{31}$$

REFERENCES

[1] E. P. Blasch and S. Plano, "JDL level 5 fusion model: User refinement issues and applications in group tracking," *Proc. SPIE*, vol. 4729, pp. 270–280, Jul. 2002.

[2] M. M. Kokara, C. J. Matheusb, and K. Baclawskic, "Ontology-based situation awareness," *Inf. Fusion*, vol. 10, no. 1, pp. 83–98, Jan. 2009.

[3] C. J. Matheus *et al.*, "SAWA: An assistant for higher-level fusion and situation awareness," *Proc. SPIE*, vol. 5813, pp. 75–85, Mar. 2005.

[4] K. Golestan, R. Soua, F. Karray, and M. S. Kamel, "Situation awareness within the context of connected cars: A comprehensive review and recent trends," *Inf. Fusion*, vol. 29, pp. 68–83, May 2016.

[5] S. J. Yang, A. Stotz, J. Holsopple, M. Sudit, and M. Kuhl, "High level information fusion for tracking and projection of multistage cyber attacks," *Inf. Fusion*, vol. 10, no. 1, pp. 107–121, Jan. 2009.

[6] K. Sycara *et al.*, "An integrated approach to high-level information fusion," *Inf. Fusion*, vol. 10, no. 1, pp. 25–50, Jan. 2009.

[7] L. Xu, Y. Liang, G. Zhou, and Z. Duan, "Route-based dynamics modeling and tracking with application to air traffic surveillance," *IEEE Trans. Intell. Transp. Syst.*, to be published. doi: 10.1109/TITS.2018.2890570.

[8] A. Aprile, E. Grossi, M. Lops, and L. Venturino, "Track-before-detect for sea clutter rejection: Tests with real data," *IEEE Trans. Aerosp. Electron. Syst.*, vol. 52, no. 3, pp. 1035–1045, Jun. 2016.

[9] L. A. Johnston and V. Krishnamurthy, "Performance analysis of a dynamic programming track before detect algorithm," *IEEE Trans. Aerosp. Electron. Syst.*, vol. 38, no. 1, pp. 228–242, Jan. 2002.

[10] S. Buzzi, M. Lops, and L. Venturino, "Track-before-detect procedures for early detection of moving target from airborne radars," *IEEE Trans. Aerosp. Electron. Syst.*, vol. 41, no. 3, pp. 937–954, Jul. 2005.

[11] J. Yan, H. Liu, B. Jiu, Z. Liu, and Z. Bao, "Joint detection and tracking processing algorithm for target tracking in multiple radar system," *IEEE Sensors J.*, vol. 15, no. 11, pp. 6534–6541, Nov. 2015.

[12] H. Lan, Y. Liang, Q. Pan, F. Yang, and C. Guan, "An EM algorithm for multipath state estimation in OTHR target tracking," *IEEE Trans. Signal Process.*, vol. 62, no. 11, pp. 2814–2826, Jun. 2014.

[13] S. Challa and G. W. Pulford, "Joint target tracking and classification using radar and ESM sensors," *IEEE Trans. Aerosp. Electron. Syst.*, vol. 37, no. 3, pp. 1039–1055, Jul. 2001.

[14] N. Gordon, S. Maskell, and T. Kirubarajan, "Efficient particle filters for joint tracking and classification," *Proc. SPIE*, vol. 4728, pp. 439–449, Aug. 2002.

[15] P. Smets and B. Ristic, "Kalman filter and joint tracking and classification based on belief functions in the TBM framework," *Inf. Fusion*, vol. 8, no. 1, pp. 16–27, Jan. 2007.

[16] X. R. Li, M. Yang, and J. Ru, "Joint tracking and classification based on Bayes joint decision and estimation," in *Proc. 10th Int. Conf. Inf. Fusion*, Quebec, QC, Canada, Jul. 2007, pp. 1–8.

[17] W. Cao, J. Lan, and X. R. Li, "Conditional joint decision and estimation with application to joint tracking and classification," *IEEE Trans. Syst., Man, Cybern. Syst.*, vol. 46, no. 4, pp. 459–471, Apr. 2016.

[18] W. Cao, M. Hui, L. Bai, and B. Yao, "Compact conditional joint decision and estimation for joint tracking and identification with performance evaluation," *IEEE Access*, vol. 6, pp. 4395–4404, 2018.

[19] T. Vercauteren, D. Guo, and X. Wang, "Joint multiple target tracking and classification in collaborative sensor networks," *IEEE J. Sel. Areas Commun.*, vol. 23, no. 4, pp. 714–723, Apr. 2005.

[20] E. P. Blasch, "Modeling intent for a target tracking and identification scenario," *Proc. SPIE*, vol. 5428, pp. 260–270, Aug. 2004.

[21] M. M. Kokar and G.-W. Ng, "High-level information fusion and situation awareness," *Inf. Fusion*, vol. 10, no. 1, pp. 2–5, Jan. 2009.

[22] C. G. Looney and L. R. Liang, "Cognitive situation and threat assessments of ground battlespaces," *Inf. Fusion*, vol. 4, no. 4, pp. 297–308, Dec. 2003.

[23] J. L. Yepes, I. Hwang, and M. Rotea, "New algorithms for aircraft intent inference and trajectory prediction," *J. Guid., Control, Dyn.*, vol. 30, no. 2, pp. 370–382, 2007.

[24] J. Krozel and D. Andrisani, "Intent inference with path prediction," *J. Guid., Control, Dyn.*, vol. 29, no. 2, pp. 225–236, 2007.

[25] A. Wang, V. Krishnamurthy, and B. Balaji, "Intent inference and syntactic tracking with GMTI measurements," *IEEE Trans. Aerosp. Electron. Syst.*, vol. 47, no. 4, pp. 2824–2843, Oct. 2011.

[26] B. I. Ahmad, J. K. Murphy, P. M. Langdon, and S. J. Godsill, "Bayesian intent prediction in object tracking using bridging distributions," *IEEE Trans. Cybern.*, vol. 48, no. 1, pp. 215–227, Jan. 2018.

[27] L. Xu, X. R. Li, and Z. Duan, "Hybrid grid multiple-model estimation with application to maneuvering target tracking," *IEEE Trans. Aerosp. Electron. Syst.*, vol. 52, no. 1, pp. 122–136, Feb. 2016.

[28] W. Mei, G. L. Shan, and X. R. Li, "Simultaneous tracking and classification: A modularized scheme," *IEEE Trans. Aerosp. Electron. Syst.*, vol. 43, no. 2, pp. 581–599, Apr. 2007.

[29] L. Xu, X. R. Li, Y. Liang, and Z. Duan, "Constrained dynamic systems: Generalized modeling and state estimation," *IEEE Trans. Aerosp. Electron. Syst.*, vol. 53, no. 5, pp. 2594–2609, Oct. 2017.

[30] K. Ito and K. Xiong, "Gaussian filters for nonlinear filtering problems," *IEEE Trans. Autom. Control*, vol. 45, no. 5, pp. 910–927, May 2000.

[31] E. A. Wan and R. Van Der Merwe, "The unscented Kalman filter for nonlinear estimation," in *Proc. ASSPCC*, Lake Louise, AB, Canada, 2000.

[32] M. S. Arulampalam, S. Maskell, N. Gordon, and T. Clapp, "A tutorial on particle filters for online nonlinear/non-Gaussian Bayesian tracking," *IEEE Trans. Signal Process.*, vol. 50, no. 2, pp. 174–188, Feb. 2002.

WANYING ZHANG received the M.S. degree from the School of Automation, Northwestern Polytechnical University, Shaanxi, China, in 2017, where she is currently pursuing the Ph.D. degree in control science and engineering. Her research interests include estimation theory, target tracking, and information fusion.

FENG YANG received the B.E., M.E., and Ph.D. degrees from Northwestern Polytechnical University (NPU), in 2000, 2003, and 2007, respectively, where he is currently an Associate Professor with the School of Automation, NPU. His research interests include information fusion and target tracking. He is a member of the Chinese Committee of Information Fusion.

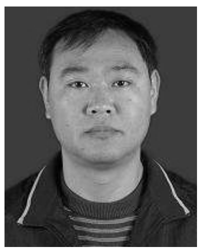

YAN LIANG received the B.E., M.E., and Ph.D. degrees from Northwestern Polytechnical University (NPU), in 1993, 1998, and 2001, respectively. He was a Postdoctoral Fellow of Tsinghua University, China, from 2001 to 2003, a Research Fellow of The Hong Kong Polytechnic University, from 2006 to 2006, and a Visiting Scholar with the University of Alberta, from 2007 to 2008. Since 2009, he has been a Professor with the School of Automation. His research interests include estimation theory, information fusion, and target tracking.